www.czasopisma.pan.pl PAN POLSKA AKADEMIA NAUK www.journals.pan.pl

Arch. Metall. Mater. **64** (2019), 4, 1269-1275

DOI: 10.24425/amm.2019.130090

G. GUMIENNY*#, B. KUROWSKA*, P. JUST*

THE EFFECT OF MANGANESE ON THE CRYSTALLISATION PROCESS, MICROSTRUCTURE AND SELECTED PROPERTIES OF COMPACTED GRAPHITE IRON

The paper presents the effect of manganese on the crystallization process, microstructure and selected properties: cast iron hardness as well as ferrite and pearlite microhardness. The compacted graphite was obtained by Inmold technology. The lack of significant effect on the temperature of the eutectic transformation was demonstrated. On the other hand, a significant reduction in the eutectoid transformation temperature with increasing manganese concentration has been shown. The effect of manganese on microstructure of cast iron with compacted graphite considering casting wall thickness was investigated and described. The nomograms describing the microstructure of compacted graphite iron versus manganese concentration were developed. The effect of manganese on the hardness of cast iron and microhardness of ferrite and pearlite were given.

Keywords: compacted graphite iron, crystallization, manganese, DTA method

1. Introduction

Until the middle of the 20th century compacted graphite iron (CGI) was considered as cast iron with unsuccessful nodular graphite. However, due to interesting properties this material is more and more willingly used by constructors [1,2].

Compacted graphite is defined in PN-EN ISO 945-1 as type III. In accordance with PN-EN 16079: 2012, the compacted graphite iron shall contain minimum 80% of graphite type III. In accordance with PN-EN ISO 945-1, the rest of precipitates can be characterized as types IV, V and VI. The shape of compacted graphite is intermediate between flake and nodular graphite. For the above mentioned reason, the mechanical properties of CGI are intermediate between grey and nodular cast iron. The mechanical properties as well as the matrix microstructure of CGI according to PN-EN 16079: 2012 are presented in table 1.

From the foregoing it follows that the minimum tensile strength is from 300 to 500 MPa, with an elongation from 2 to 0.5%, respectively. Tab. 1 also shows that the standard does not provide for a completely ferritic matrix despite the fact that CGI has a high tendency to form ferrite.

Relatively high mechanical properties and good thermal conductivity make this material more and more popular among manufacturers of high quality castings. In comparison to cast iron with flake graphite CGI is characterized by higher strength properties, higher elongation, corrosion resistance and low section sensitivity. Compared to ductile cast iron it is characterized by higher thermal shock resistance, higher thermal conduction, better damping capacity as well as better castability. Undoubted advantage of CGI is relatively low production cost in comparison to ductile iron resulting from less consumption of a master alloy [3,4]. Due to the large contact surface of graphite with the matrix, CGI tends to form ferrite both directly and indirectly [3].

Manganese is one of the basic elements in cast iron. In the liquid state it dissolves in it without restrictions. Above a concentration of approx. 1.2% it is considered as an alloying element.

TABLE 1

The grades of CGI according to PN-EN 16079:2012

Symbol	Mechanical properties				Matrix microstructure
	R_m, MPa min.	$R_{p0,2}$, MPa min.	A, % min.	HBW	
EN-GJV-300	300	210	2.0	140 to 210	predominantly ferritic
EN-GJV-350	350	245	1.5	160 to 220	ferritic-pearlitic
EN-GJV-400	400	280	1.0	180 to 240	pearlitic-ferritic
EN-GJV-450	450	315	1.0	200 to 250	predominantly pearlitic
EN-GJV-500	500	350	0.5	220 to 260	fully pearlitic

* LODZ UNIVERSITY OF TECHNOLOGY, DEPARTMENT OF MATERIALS ENGINEERING AND PRODUCTION SYSTEMS, 1/15 STEFANOWSKIEGO STR., 90-924 ŁÓDŹ, POLAND

Corresponding author: grzegorz.gumienny@p.lodz.pl

Its maximum concentration in cast iron for non-magnetic castings and resistant to gases and chemicals is ~20%. Manganese is carbide-forming element, at a concentration greater than 0.7% it is possible to crystallization carbides on the eutectic grains boundaries [5]. Mn reduces the temperature range of the eutectic transformation according to a stable and metastable system. It causes the shift of the eutectic transformation point to the right but the eutectoid to the left. Manganese increases the stability of austenite. It is a pearlite forming element too [6]. Mn dissolves in cementite to form (Fe,Mn_3C). There are discrepancies regarding the effect of manganese on a cast iron graphitization. Some authors reports that at the concentration of 0.8-1.2% there is no effect, other publications indicate that it is carbide forming element in the entire concentration range. Manganese promotes the formation of interdendritic graphite separations. According to A. Roula manganese makes degeneracy in nodular graphite [7]. To a concentration of approx. 1.2%, Mn increases hardness, tensile strength and decrease in an elongation. It also has an adverse effect on the cast iron properties by increasing its shrinkage and brittleness.

The above-mentioned information shows that there are many data concerning the impact of manganese on the microstructure and properties of cast iron [6-16]. However, there are still literature deficiencies regarding the manganese impact in cast iron with compacted graphite. In particular, they concern the joint influence of manganese and the casting wall thickness on CGI microstructure. The shortcomings in this field prompted the Authors to complete the data in this research area.

2. Materials and methods

The tested cast iron was melted in a medium frequency induction furnace with a crucible of 30 kg capacity. The furnace charge consisted of special pig iron with a maximum sulphur concentration of 0.01%, ferro-silicon and ferro-manganese. The superheat temperature amounts to approx. 1530°C while the pouring temperature – 1480°C. The compacted graphite was obtained using Inmold technology. The schematic layout of elements in the mould is presented in Figure 1.

In a spherical reaction chamber (3) the magnesium master alloy LAMET 5504 with chemical composition presented in table 2 was placed. For the better mixing of the master alloy with liquid cast iron, a spherical mixing chamber (4) was placed behind the reaction chamber. There was also a control chamber (5) behind the mixing chamber. In its thermal center, an S-type thermocouple was placed. The voltage signal from the thermocouple went to the U/f frequency converter through the compensating cable. Then the signal went to the computer, where curves of the differential thermal analysis (DTA) were recorded. This made it possible to assess the effect of manganese on the temperature of phase transformations in CGI. The stepped test casting (6) was characterized by the wall thickness 3, 6, 12 and 24 mm. It allows to test the influence of the wall thickness (cooling rate) on the cast iron microstructure.

TABLE 2

The chemical composition of the master alloy

Chemical composition, wt%					
Si	**Mg**	**Ca**	**La**	**Al**	**Fe**
44-48	5-6	0.4-0.6	0.25-0.40	0.8-1.2	rest

Magnesium and lanthanum are nodulizers in the master alloy. There are also calcium and aluminum as inoculants, while silicon is a graphite-forming element. The dose of master alloy was calculated based on the assumed final magnesium concentration in the casting – 0.017%. The average Mg concentration in the master alloy was assumed at 5.5%. The assuming magnesium yield was 80%. Knowing the mass of the processed metal, a portion of the master alloy was set at 19.8 g.

From the central parts of the stepped casting, specimens for metallographic examinations were cut out. Using a Nikon MA200 metallographic microscope, the microstructure was

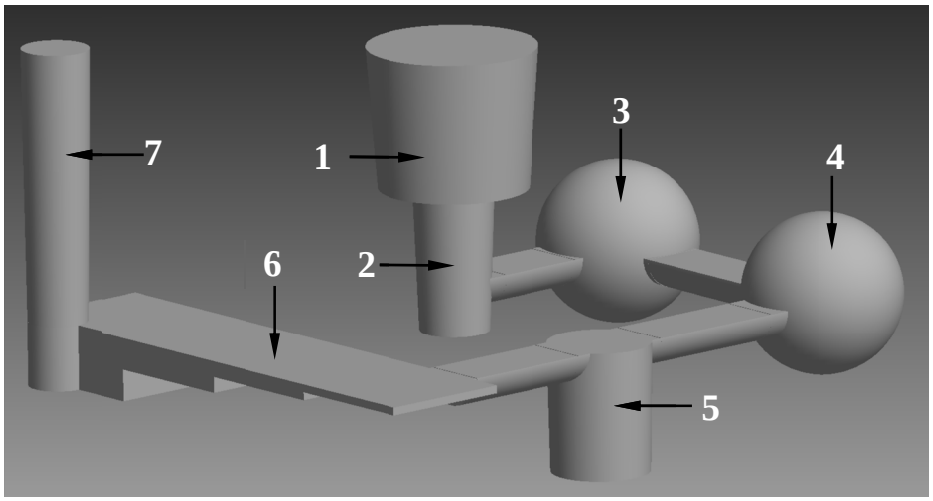

Fig. 1. Schematic layout of elements in the mould: 1 – pouring cup, 2 – downsprue, 3 – reaction chamber, 4 – mixing chamber, 5 – control chamber, 6 – stepped test casting, 7 – flow – off

examined at a magnification of ×500 on microsections etched with 4% solution of nitric acid in ethyl alcohol. The fraction of individual phases was determined with the NIS Elements BR (Basic Research) program. The cast iron chemical composition was tested with a SPECTROMAXx arc spark OES metal analyser and it is shown in table 3.

TABLE 3

The chemical composition of CGI tested

No.	Chemical composition, wt%					
	C	Si	Mn	Mg	P	S
1.	3.72	2.48	0.04	0.019	0.06	0.010
2.	3.87	2.43	0.27	0.022	0.05	0.008
3.	3.69	2.58	0.58	0.020	0.06	0.009
4.	3.70	2.45	0.89	0.018	0.07	0.011
5.	3.82	2.43	1.04	0.017	0.05	0.009
6.	3.84	2.41	1.39	0.016	0.05	0.010

The scope of the chemical composition was dictated by the increasing tendency for crystallization according to a metastable system, especially thick-walled castings.

The cast iron hardness was examined on the specimens from castings with the wall thickness of 24 mm with an HPO-2400 hardness tester under the conditions: 187.5/2.5/30. The microhardness tests were performed on the HV-1000B microhardness tester under a load of 0.9807 N according to PN EN ISO 6507-1.

3. Results

Figure 2 (a, b) shows the DTA curves of CGI containing 0.04% Mn.

The first thermal effect comes from the primary austenite crystallization and it is described as AB. The second thermal effect comes from the eutectic mixture (austenite + compacted graphite) crystallization. It is described as DEFH. The temperature recalescence (tF – tD) is 5°C. The end of eutectic transformation denotes the end of cast iron crystallization and it occurs at 1107°C (point H, Fig. 2a). Figure 2b shows the transformation in the solid state. The austenite transformation starts at 778°C (point K) from the $\gamma \rightarrow \alpha$ transformation. The end of solid state transformation marked "M" occurs at 723°C.

Figure 3 (a, b) shows DTA curves of cast iron containing 1.39% Mn.

The maximum eutectic transformation temperature (tF) occurs at 1153°C and it is 3°C higher compared to cast iron containing 0.04% Mn. The eutectic crystallization occurs at 1108°C and it was similar to the previously described case. The austenite transformation starts at 749°C. It means that the temperature was lower by 29°C compared to CGI containing 0.04% Mn. The austenite transformation finish occurred at 691°C. It means that the temperature was lower by 32°C lower compared to the previously described cast iron. Therefore, no significant effect of manganese on the temperature range of the solid state transformation was found.

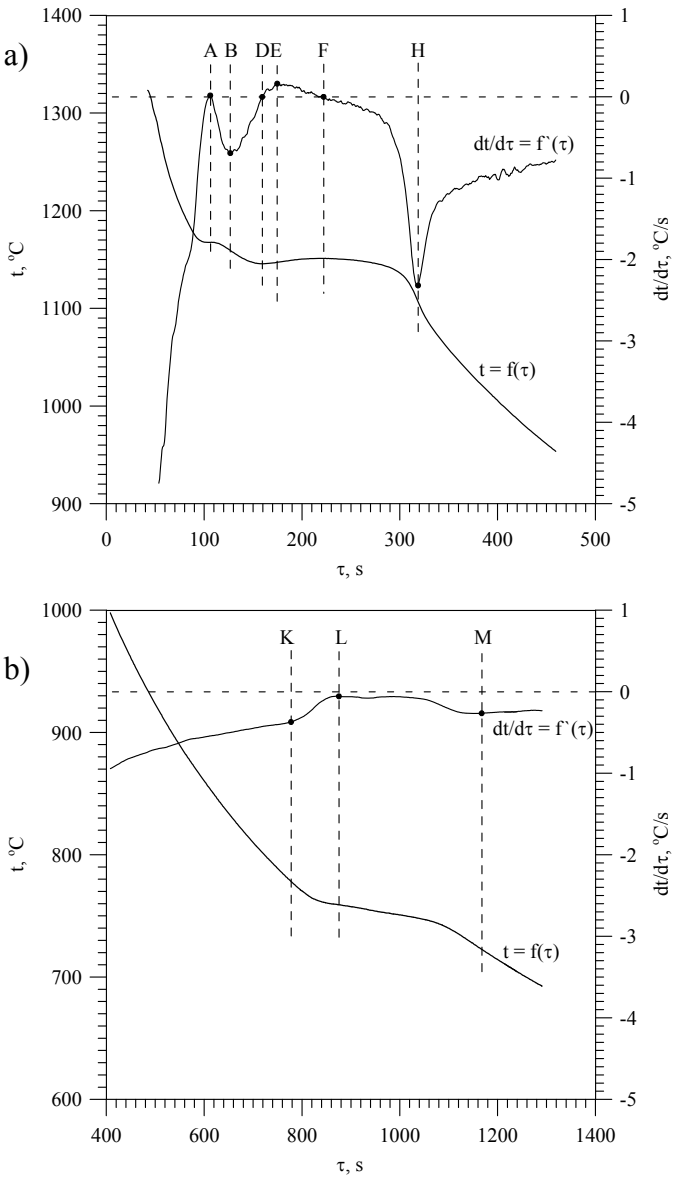

Point	τ, s	t, °C	dt/dτ, °C/s
A	106	1167	0.01
B	127	1159	–0.69
D	160	1146	0
E	175	1147	0.16
F	222	1150	0
H	319	1107	–2.32
K	778	778	0.37
L	876	759	–0.06
M	1167	723	–0.27

Fig. 2 (a, b). DTA curves of CGI containing 0.04% Mn: a) in the crystallization area b) in the austenite transformation area

Figures 4 and 5 show, the effect of manganese on the temperature of the eutectic transformation and the temperature of the austenite transformation, respectively.

The data presented in Fig. 4 show that Mn slightly increases the crystallization temperature of graphite eutectic in CGI. However, this impact should be considered negligible. A significant effect of Mn on the temperature of the transformation in the solid

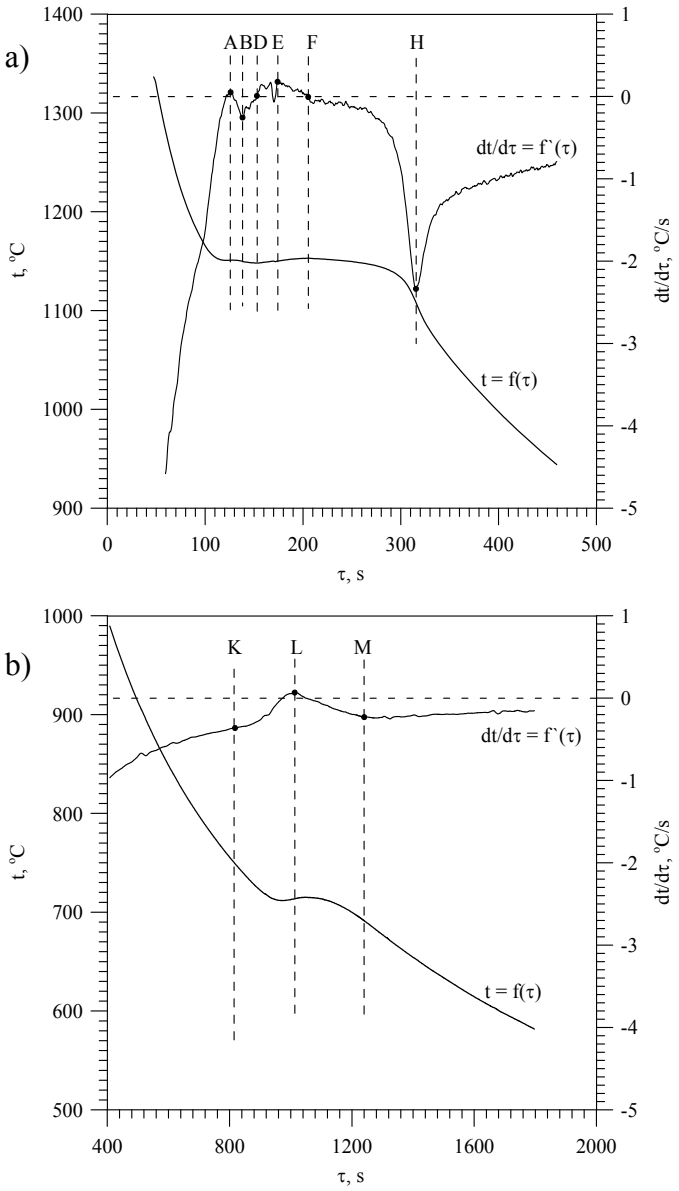

Point	τ, s	t, °C	$dt/d\tau$, °C/s
A	126	1151	0.05
B	138	1150	–0.26
D	153	1148	0
E	174	1150	0.18
F	205	1153	0
H	316	1108	–2.34
K	818	749	–0.36
L	1013	714	0.07
M	1240	691	–0.23

Fig. 3 (a, b). DTA curves of CGI containing 1.39% Mn: a) in the crystallization area b) in the austenite transformation area

state was demonstrated (Fig. 5). Every 1% of the manganese decreases the starting temperature of the solid state transformation in CGI by about 23°C and the end temperature by about 26°C in the tested range of the chemical composition. Most literature references determine this decrease at approximately 35°C per 1% concentration.

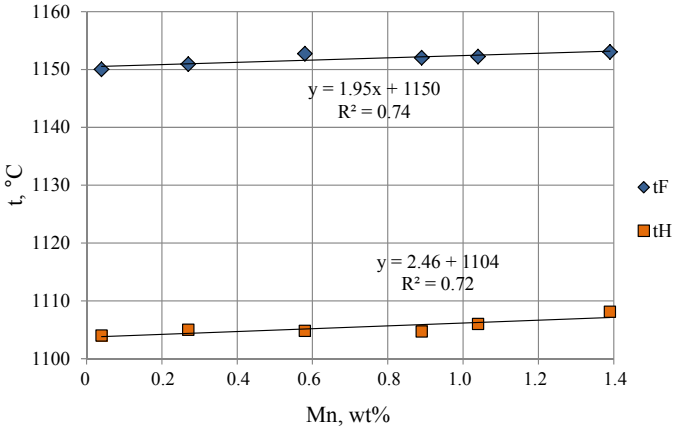

Fig. 4. Eutectic transformation temperature vs. manganese concentration

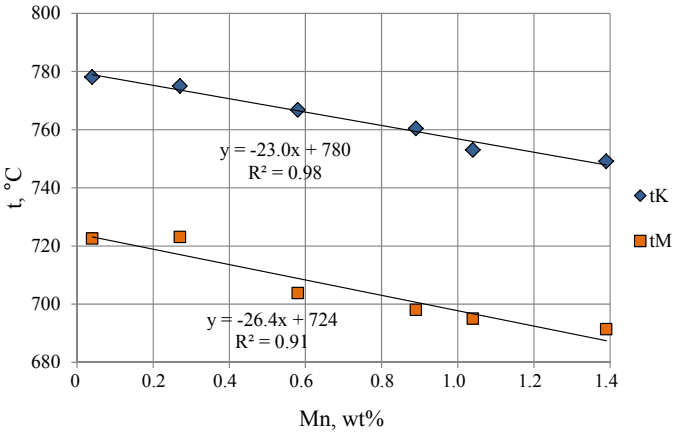

Fig. 5. Austenite transformation temperature vs. manganese concentration

Figure 6 shows the microstructure of CGI containing 0.04% Mn in castings with the wall thickness 3 (a) and 24 mm (b).

In thin-walled castings (Fig. 6a) the matrix composition is as follows: pearlite 70%, ferrite 30%. There was no cementite precipitations. In the thick-wall castings (24 mm), the proportions of ferrite and pearlite are reversed – the volume fraction of ferrite is ~70% while perlite ~30%. As the casting wall thickness increases, the number of graphite precipitates decreases, while their average size increases. This is due to the obvious effect of the cooling rate on the rate of the nucleation.

Figure 7 (a, b) shows the microstructure of CGI containing 0.58% Mn with the wall thickness 3 (a) and 24 mm (b).

In castings with a wall thickness of 3 mm, the cementite volume fraction was estimated at 7%. The volume fraction of pearlite increased to about 80%, the rest was occupied by ferrite (~13%). The cementite was also observed in castings with a wall thickness of 6 mm. Fig. 7b shows that the perlite volume fraction in the matrix is about 55%.

Figure 8 (a, b) shows the microstructure of CGI containing 1.39% Mn with the wall thickness 3 (a) and 24 mm (b).

Cast iron containing 1.39% Mn in castings with the wall thickness of 3 mm cannot be called CGI due to the high volume fraction of $(Fe, Mn)_3C$ (~37%). The amount of cementite in

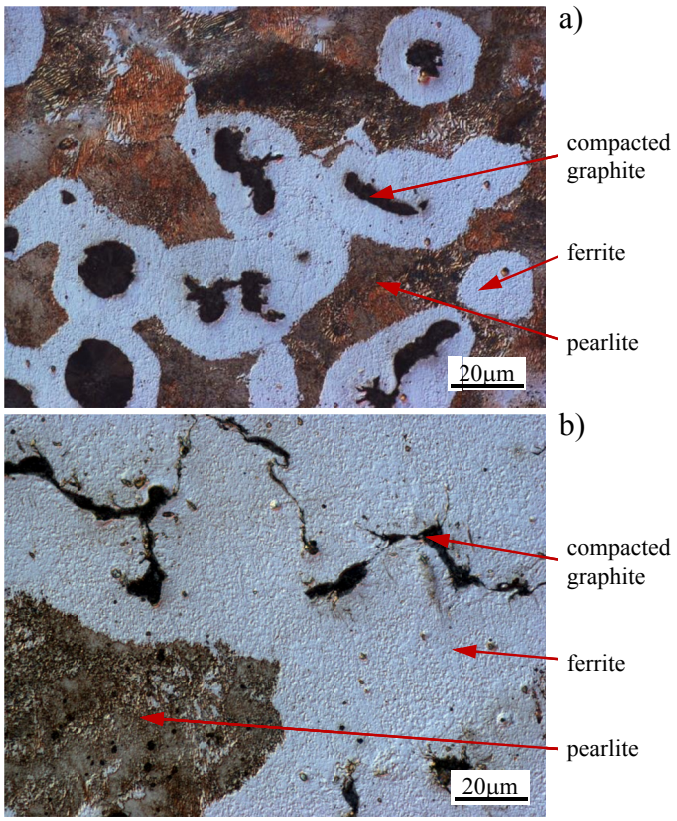

Fig. 6 (a, b). Microstructure of CGI containing 0.04% Mn in castings with the wall thickness 3 mm (a) and 24 mm (b): compacted graphite, ferrite, pearlite

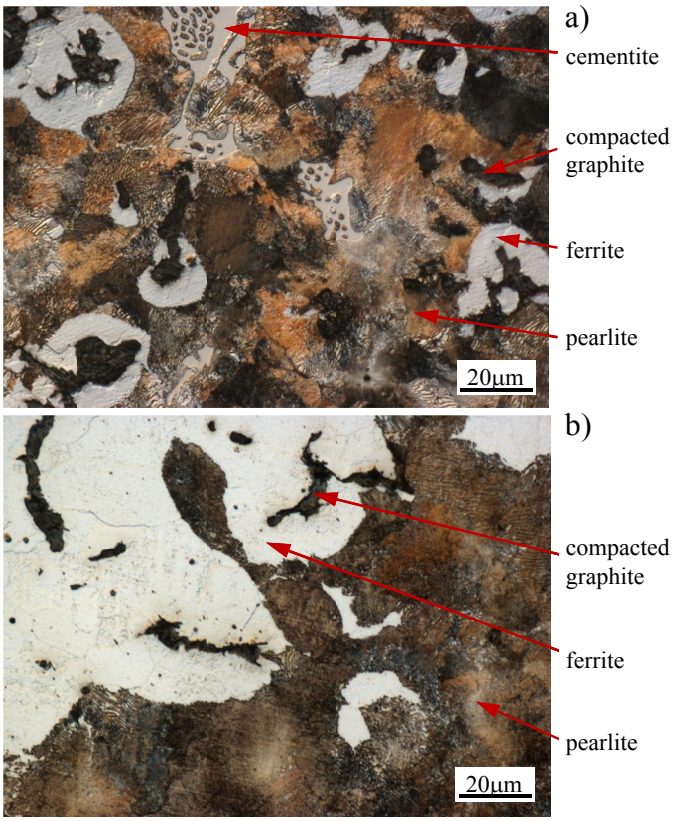

Fig. 7 (a, b). Microstructure of CGI containing 0.58% Mn in castings with the wall thickness 3 mm (a) and 24 mm (b): compacted graphite, pearlite, ferrite, cementite (only Fig. 7a)

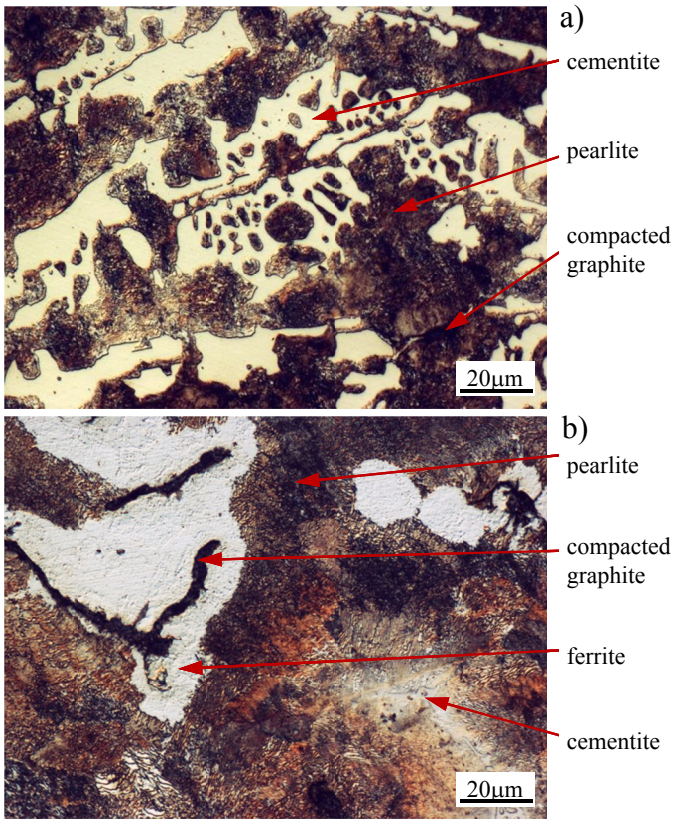

Fig. 8 (a, b). Microstructure of CGI containing 1.39% Mn in castings with the wall thickness 3 mm (a) and 24 mm (b): compacted graphite, pearlite, cementite, ferrite (only Fig. 8b)

castings with the wall thickness of 6 mm decreased to ~11%. The remaining part of the matrix was predominantly pearlitic.

With the increase in the Mn concentration, the pearlite surface area increased in the casting with the wall thickness of 6-24 mm. In castings with the wall thickness of 3 and 6 mm the carbides precipitated at a concentration of approx. 0.58% Mn, in a casting of 12 mm – at a concentration of ~1% Mn, while in castings with the thickness of 24 mm, cementite was observed only in cast iron containing 1.39% Mn.

CGI microstructure components vs. manganese concentration in castings with the wall thickness of 3, 6, 12 and 24 mm are presented in Figure 9 (a-d).

Fig. 9a shows that in castings with the wall thickness of 3 mm, manganese should be considered as a carbide-forming element. The decrease in the ferrite volume fraction is mainly related to the increase in the cementite volume fraction; the amount of pearlite does not change significantly. The situation is different in castings with the wall thickness of 6-24 mm, where Mn should be considered as a pearlite-forming element despite the fact that in the castings with the wall thickness of 6 mm the volume fraction of cementite was significant. The developed nomograms can be useful for estimating the components of CGI microstructure vs. Mn concentration and the casting wall thickness.

Table 4 shows the effect of Mn on the ferrite and pearlite microhardness, while Figure 10 shows the effect of the Mn on the pearlite microhardness. The hardness of CGI vs. manganese concentration is presented in Figure 11.

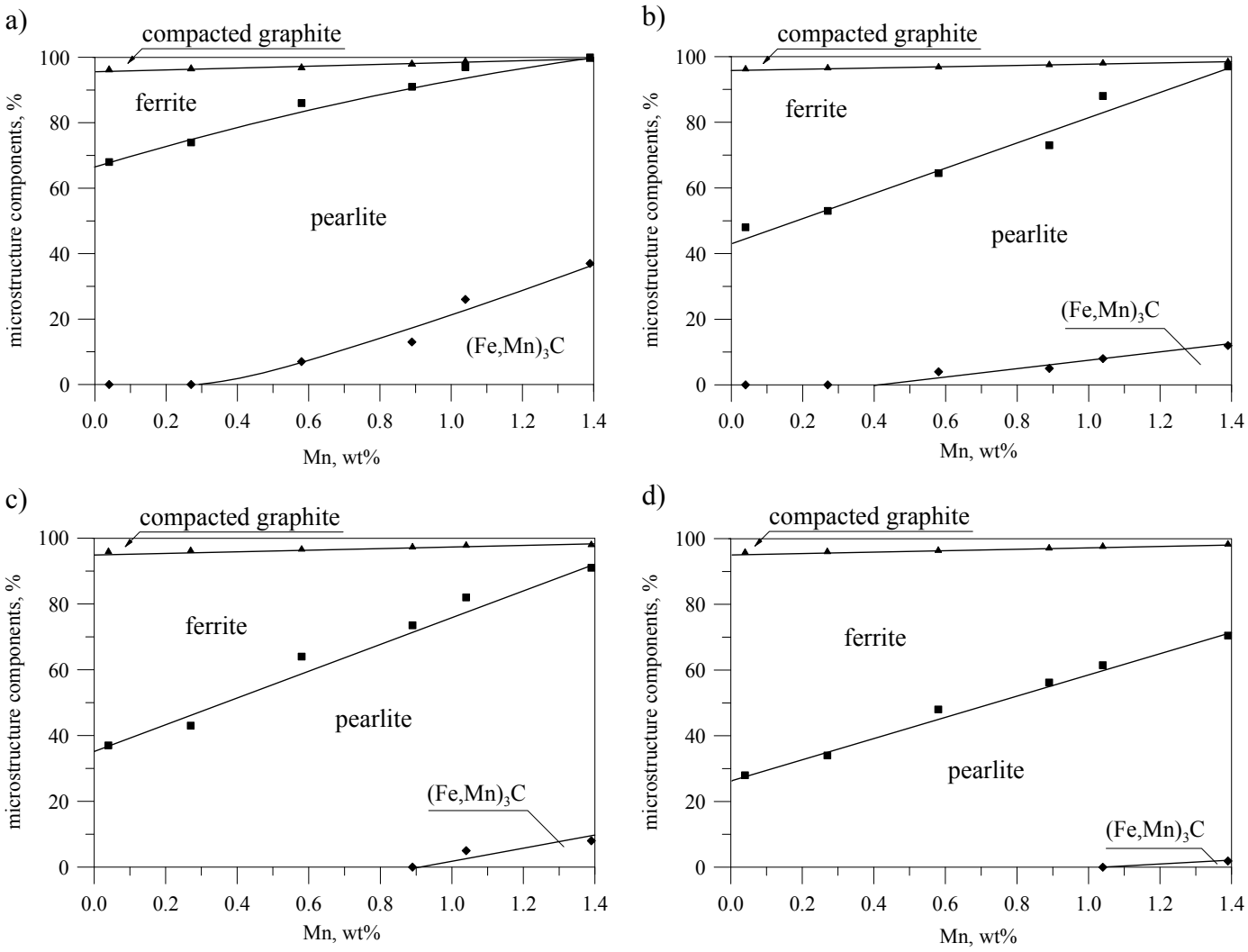

Fig. 9 (a-d). CGI microstructure components vs. manganese concentration in castings with the wall thickness: a) 3 mm, b) 6 mm, c) 12 mm, d) 24 mm

From the data presented in Fig. 10 and 11 it follows that manganese increases perlite microhardness by approx. 34 µHV0.1 per 1% Mn while CGI hardness by approx. 63 HB per 1%. There was no significant effect of manganese on the microhardness of ferrite. It follows that the pearlite microhardness increases as a result of the dissolution of manganese in the cementite and the increase of its microhardness.

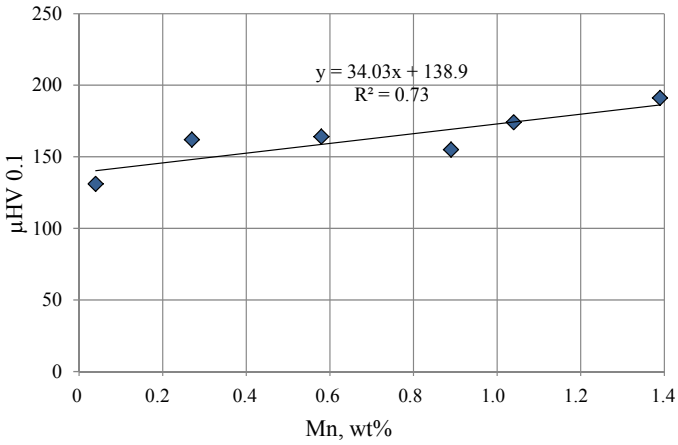

Fig. 10. Pearlite microhardness vs. Mn concentration

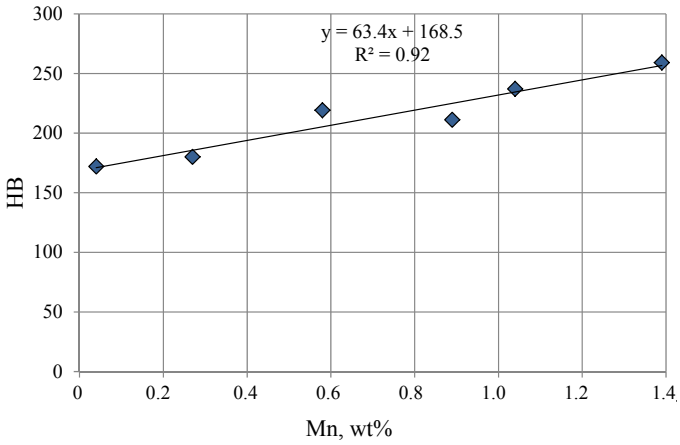

Fig. 11. CGI hardness vs. Mn concentration

TABLE 4

Pearlite and ferrite microhardness vs. Mn concentration

Mn, wt%	Microhardness, mHV0.01	
	ferrite	pearlite
0.04	89	131
0.27	91	162
0.58	92	164
0.89	87	155
1.04	90	174
1.39	92	191

4. Conclusion

From the data included in this paper the following conclusions can be drawn:

- every 1% of the manganese decreases the starting temperature of the solid state transformation in CGI by about 23°C and the end temperature by about 26°C,
- in thin-walled castings, manganese is a carbide-forming element (it promotes the formation of cementite from the liquid), whereas in thick-walled castings it is a pearlite-forming element,
- the addition of manganese in compacted graphite iron does not result in obtaining a fully pearlitic metal matrix in castings with a wall thickness of 3-24 mm,
- every 1% increase in manganese concentration increases the CGI hardness by about 63 HB, in thick-walled castings it is caused by an increase in the volume fraction of pearlite.

REFERENCES

[1] S. Dawson, Compacted graphite iron – A material solution for modern diesel engine cylinder blocks and heads, China Foundry **6** (3), 241-246 (2009).

[2] E.E.T. ELSawy, M.R. EL-Hebeary, I.S.E. El Mahallawi, Effect of manganese, silicon and chromium additions on microstructure and wear characteristics of grey cast iron for sugar industries applications, Wear **390-391**, 113-124 (2017),

[3] S. Pietrowski, Compendium of knowledge about compacted graphite iron. Solidifications of Metals and Alloys **44**, 279-292 (2000).

[4] M.S. Soiński, A. Jakubus, Initial Assessment of Abrasive Wear Resistance of Austempered Cast Iron with Vermicular Graphite, Archives of Metallurgy and Materials **59** (3), 1073-1076 (2014).

[5] A. Nayar, The metals databook, Tata McGraw-Hill Education (1997).

[6] L. Rao, W. Tao, S. Wang, M. Geng, Influence of the composition ratio of manganese and copper on the mechanical properties and the machining performance of ductile iron. Indian Journal of Engineering & Materials Sciences **21**, 573-579 (2014)

[7] A. Roula, G.A. Kosnikov, Manganese distribution and effect on graphite shape in advanced cast irons. Materials Letters **62**, 3796-3799 (2008).

[8] O. Agunsoye, E.F. Ochulor, S.I. Talabi, S. Olatunji, Effect of Manganese Additions and Wear Parameter on the Tribological Behaviour of NFGrey (8) Cast Iron, Tribology in Industry **34** (4), 239-246 (2012).

[9] S. Dymek, M. Blicharski, E. Fraś, Synthesis of Nanoparticles in The Ferrite of Ductile Iron, Archives of Metallurgy and Materials **52** (1), 129-134 (2007).

[10] S. Hiratsuka, H. Horie, T. Kowata, K. Koike, K. Shimizu, Influence of Steel Scrap on Microstructure and Mechanical Properties of Spheroidal Graphite Cast Iron, Materials Transactions **44** (7), 1419-1424 (2003).

[11] M.J. Kadhim, A.N. Abood, R.S. Yaseen, The Role of Manganese on Microstructure of High Chromium White Cast Iron, Modern Applied Science **5** (1), 179-185 (2011).

[12] R. Gundlach, M. Meyer, L. Winardi, Influence of Mn and S on the Properties of Cast Iron Part III – Testing And Analysis, International Journal of Metalcasting **9** (2), 69-82 (2015).

[13] L. Rao, W.-W. Tao, S.-J. Wang, M.-P. Geng, G.-X. Cheng, Influence of the composition ratio of manganese and copper on the mechanical properties and the machining performance of ductile iron, Indian Journal of Engineering and Materials Sciences **21** (5) 573-579 (2014).

[14] K.M. Ahmad, M.R. Maarof, M. Ishak, M.S. Huzairi, Microstructure and Mechanical Properties of Austenitic Compacted Cast Iron with Additive Manganese, MATEC Web of Conferences **74** (00009), (2016).

[15] A.K. Muzafar, M.M. Rashidi, I. Mahadzir, Z. Shayfull, Effect on Mechanical Properties of Heat Treated High Manganese Austenitic Cast Iron, MATEC Web of Conferences **78** (01081), (2016).

[16] D. Medyński, A. Janus, B. Samociuk, J. Chęcmanowski, Effect of Microstructures on Working Properties of Nickel-Manganese-Copper Cast Iron, Metals **8** (341), 1-12 (2018).